Theory of nuclear reactions involving halo nuclei

J. A. Tostevin*[a]

[a]Department of Physics, University of Surrey, Guildford, Surrey, GU2 5XH, U.K.

Adiabatic and eikonal theoretical methods being developed for and applied to halo nucleus-target scattering and reactions are outlined. Approximation schemes which were adequate for calculations of reaction cross sections in collisions of tightly bound nuclei are shown to be inadequate when applied to loosely bound extended halo nuclei. Few-body calculations of angular distributions for ^{8}He and ^{11}Be scattering are also discussed and the treatment and importance of non-eikonal corrections are investigated.

1. INTRODUCTION

In nuclear fragmentation reactions light nuclei with exotic combinations of neutrons and protons are produced which extend to the very limits of nuclear stability – the neutron and proton driplines. These nuclei display new physical phenomena, such as the neutron halo, and are most effectively treated as a highly correlated motion of a relatively few constituent bodies. Unlike stable ($N \approx Z$) nuclei which possess well developed excited state spectra and are thus amenable to a variety of spectroscopic methods and tools, dripline nuclei often possess a single (particle stable) bound state. Halo nucleus sizes and structures must therefore be deduced indirectly from their cross sections and responses to strong and electromagnetic probes. These deductions require practical quantitative quantum mechanical calculations for the structures and reactions of such few-body systems.

In this paper we review briefly the assumptions underlying eikonal treatments of the interactions between composite nuclei. We show that these methods offer a theoretical framework from which to develop calculations of reactions of loosely bound few-body composites such as halo nuclei. We first discuss briefly recent work [1–3] which reveals the importance of an explicit treatment of the few-body nature of halo nuclei for calculations of reaction cross sections at high energies ($\approx$ 800 MeV per nucleon) – and hence for values of the matter radii of halo nuclei deduced from comparisons with experiment. We then consider the rôle of these few-body degrees of freedom in calculations of composite projectile scattering at lower projectile energies, presenting six-body calculations of ^{8}He scattering at 60 MeV per nucleon and three-body calculations of ^{11}Be scattering at 50 MeV per nucleon. In the latter case we present a prescription for including the leading order corrections to the lowest order eikonal theory for few-body projectiles. We show that such corrections are readily applied and are necessary at incident energies of order 50 MeV per nucleon and below.

*The financial support of the United Kingdom Engineering and Physical Sciences Research Council (EPSRC) in the form of Grant No. GR/J95867 is gratefully acknowledged

2. ADIABATIC AND EIKONAL APPROXIMATIONS

Accurate coupled channels schemes have been developed for treating the effects of continuum coupling in the scattering of a weakly bound two-body composite, e.g. [4]. It is doubtful however whether such methods will ever offer practical calculations for more complex systems. These coupled channels methods have however provided an assessment of more efficient adiabatic methods which offer practical approximate calculations for two-body projectiles [5] and have very recently been reported for three-body projectiles [6]. In turn, these adiabatic calculations provide an assessment of more efficient eikonal methods such as will be discussed here. Eikonal models have now been applied extensively for the calculation of angular and breakup momentum distributions of projectiles with a dominantly two- or three-body structure, such as ^{11}Li [7–9], ^{8}B [10], ^{11}Be [11] and ^{14}Be [12].

For a point particle (j) being scattered from a target nucleus by a central interaction V_j the eikonal approximation to the elastic S-matrix is [13]

$$S_j(b) = \exp[i\chi_j(b)] \quad , \qquad \chi_j(b) = -\frac{1}{\hbar v}\int_{-\infty}^{\infty} V_j(\sqrt{b^2+z^2})dz \quad , \tag{1}$$

where v is the asymptotic relative velocity and the z-axis is in the incident beam direction. χ_j, referred to as the eikonal phase, is the integral of the interaction along the assumed straight line path of the particle at an impact parameter b.

For a composite projectile, in addition to the straight line trajectory approximation, *all* eikonal approaches start from the assumption that the motions of the particles internal to the projectile (and target) are slow compared to the relative motion of their centres of mass – the adiabatic or sudden approximation limit. For an assumed n-body composite projectile p, with ground state $|\Phi_0^{(n)}\rangle$, the projectile-target elastic S-matrix for projectile centre of mass impact parameter b is then [13]

$$S_p(b) = \langle\Phi_0^{(n)}|\prod_{j=1}^{n} S_j(b_j)|\Phi_0^{(n)}\rangle \quad . \tag{2}$$

where, as above, each S_j is the elastic S-matrix for constituent j *scattering independently* from the target at its individual impact parameter b_j.

3. REACTION CROSS SECTION CALCULATIONS

Until very recently, halo nucleus matter radii and hence halo sizes have been deduced by comparing interaction or reaction cross section measurements made at high energy [14,15] with model calculations which use the optical limit (OL) of the eikonal theory [16]. The OL approximation computes S_p using Eq. (1), replacing the full projectile-target two-body interaction V_p by the single scattering '$t\rho\rho$' approximation to the multiple scattering expansion for the nucleus-nucleus optical potential [17], that is

$$V_p(R) = \int d\boldsymbol{r}_1 \int d\boldsymbol{r}_2\, \rho_p(r_1)\, \rho_t(r_2) t_{NN}(|\boldsymbol{R}+\boldsymbol{r}_1-\boldsymbol{r}_2|) \quad . \tag{3}$$

For an absorptive zero-range nucleon-nucleon (NN) amplitude and a $T=0$ target,

$$t_{NN}(\boldsymbol{r}) = (\hbar v \bar{\sigma}_{NN}/2i)\delta(\boldsymbol{r}) \quad , \tag{4}$$

where $\bar{\sigma}_{NN}$ is the average of the free nn and np total cross sections at the appropriate relative velocity. Calculation of S_p^{OL} and the reaction cross section thus involves only the projectile and target ground state densities, ρ_p and ρ_t, and neglects correlations between constituent nucleons in the projectile or target [17]. This formulation has been assessed and found to be reliable for both nucleon-nucleus and nucleus-nucleus collisions of regular (well bound) nuclear systems at sufficiently high energies, e.g. [18].

The OL approximation of uncorrelated particle motions is inappropriate given the loosely bound few-body (FB) character of halo nuclei. In the FB approach, with its adiabatic basis, Eq. (2) dictates that the scattering should be calculated for all possible configurations of the constituent particles and the resulting position dependent scattering amplitudes then weighted by the projectile ground state probability density. Since the projectile core- and valence nucleon-target two-body systems are well localised, these sub-systems *can* reasonably be treated using the OL framework. For an assumed n-body projectile at high energy therefore [1,2]

$$S_p^{FB}(b) \approx \langle \Phi_0^{(n)} | \prod_{j=1}^{n} S_j^{OL}(b_j) | \Phi_0^{(n)} \rangle \quad .$$

Reaction cross sections calculated using the FB and OL approaches when using realistic theoretical inputs [1,2] are shown in Figure 1 for ^{11}Li, ^{11}Be and ^{8}B projectiles; all at 800 MeV per nucleon incident energy on a ^{12}C target. We calculate the reaction cross sections according to

$$\sigma_R = 2\pi \int_0^\infty db\, b \left[1 - |S_p(b)|^2 \right] \quad ,$$

using Eq. (4) and the free NN cross section parameterisation of [19].

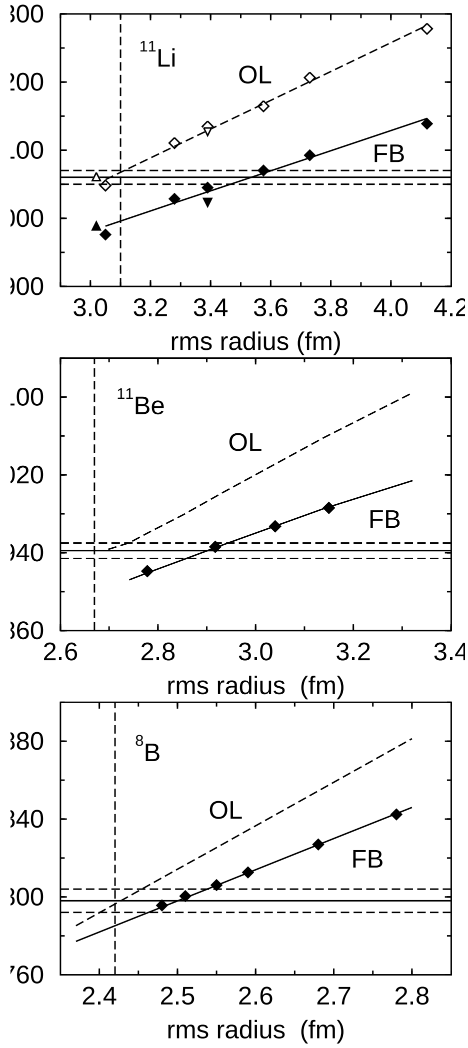

Figure 1. OL and FB calculations of reaction cross sections

Figure 1 shows the results of OL and FB calculations using a number of assumed two- and three-body wavefunctions for the projectiles. We show the calculated cross sections versus the projectile rms matter radii. The horizontal bands show the experimental datum and error in each case, $\sigma(^{11}\text{Li}) = 1060 \pm 10$ mb [20], $\sigma(^{11}\text{Be}) = 942 \pm 8$ mb [15], $\sigma(^{8}\text{B}) = 798 \pm 6$ mb [2]. The (lower) full symbols and/or solid lines are the results of the FB calculations for different wavefunction models.

The (upper) open symbols and/or dashed lines are the OL calculations using the projectile density ρ_p calculated from the same wavefunctions. We see that the correlated granular structure of the projectiles, included explicitly in the FB approach, reduces considerably the calculated reaction cross sections compared to OL estimates and thus increases significantly the values of rms matter radii deduced from the experimental data. Deduced matter rms radii for ^{11}Li and ^{11}Be, 3.53 ± 0.10 fm and 2.90 ± 0.05 fm, are increased by 14.0% and 7% over the OL values (vertical lines). The radius for ^{11}Li is consistent with models with a significant $1s$-wave intruder state component and that for ^{11}Be is consistent with models which include core excitation and reorientation [2].

4. ELASTIC SCATTERING OF HALO NUCLEI

We now turn our attention to calculations of elastic scattering of few-body projectiles at energies of between 30 and 100 MeV per nucleon. At these lower energies the reaction mechanisms are more complex and the OL theory is not an adequate basis even for the determination of the underlying projectile constituent-target interactions. At these energies the interactions in the two-body subsystems are deduced, as far as possible, from empirical data and established theoretical models for stable nuclei.

4.1. Application to ^{8}He elastic scattering

We present a new application of the FB eikonal model to ^{8}He+^{12}C scattering, an assumed α+4n+target six-body problem. We compare our calculations with new measurements of the quasielastic cross section angular distribution for this system at 60 MeV per nucleon incident energy [21]. Details of the experimental setup are given in [22].

^{8}He is the lightest nuclear system to display a neutron skin, as opposed to a very dilute one- or two-neutron halo. In ^{8}He the four valence neutrons are assumed to move about a localized α particle core. The cluster orbital shell model approximation (COSMA) wavefunction for ^{8}He [23] suggests an rms n-α separation of 3.5 fm, compared to the α rms matter radius of 1.45 fm, and thus generates a two component ground state density. ^{8}He can therefore be thought of as a prototype for reaction studies of heavier neutron dripline systems with a many-neutron skin.

The amplitude for elastic scattering of the ^{8}He composite through angle θ is [13]

$$f_{el}(\theta) = -iK \int_0^\infty db\, b\; J_0(qb)\, [S_8(b) - 1] \quad , \tag{5}$$

an integral over impact parameters b of the projectile's centre of mass. Here $q = 2K\sin(\theta/2)$ is the momentum transfer with K the incident wavenumber in the c.m. frame. A discussion of the treatment of the Coulomb interaction within the eikonal model can be found elsewhere [8]. Here we assume the Coulomb interaction acts at the projectile c.m.

The composite nature of the assumed five-body projectile appears through the eikonal S-matrix $S_8(b)$ which, from Eq. (2), is

$$S_8(b) = \langle \Phi_0^{(5)} | S_\alpha(b_\alpha) \prod_{i=1}^{4} S_i(b_i) | \Phi_0^{(5)} \rangle \quad , \tag{6}$$

where $|\Phi_0^{(5)}\rangle$ is the projectile ground state. The interactions V_j $(j = \alpha, 1, \ldots, 4)$ of the α and four neutrons $(i = 1, \ldots 4)$ with the target enter through their eikonal S-matrices, computed at each impact parameter b_j (see Figure 2) according to Eq. (1).

To compute the spatial integrals involved in Eq. (6) we make use of random sampling integration. In this study we use the harmonic oscillator based COSMA wavefunction for ^{8}He [23] which provides an analytic expression for the spin integrated four-neutron correlation function

$$\langle \Phi_0^{(5)} | \Phi_0^{(5)} \rangle_{spin} = f_{corr}(\boldsymbol{r}_1, \boldsymbol{r}_2, \boldsymbol{r}_3, \boldsymbol{r}_4)$$

entering Eq. (6) and includes correlations associated with the antisymmetrisation of the four valence neutrons, each in an assumed $p_{3/2}$ oscillator orbital with respect to the α core.

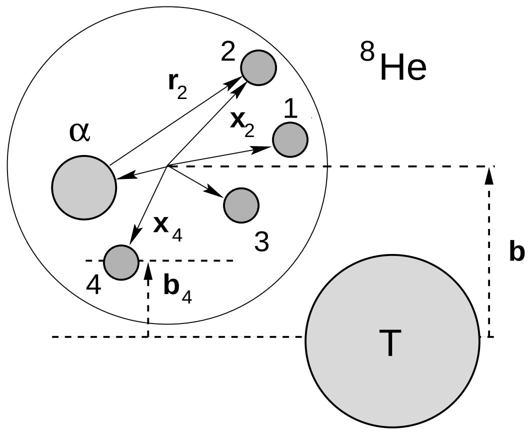

Figure 2. ^{8}He+target coordinates

f_{corr} is given explicitly in [23] where the $\boldsymbol{r}_i$ are the position vectors of the neutrons relative to the α core, see Figure 2.

The calculations sample at random the four neutron positions $\boldsymbol{r}_i$ at each ^{8}He c.m. impact parameter b. The positions $\boldsymbol{x}_\alpha = -\sum_{i=1}^{4} m_n \boldsymbol{r}_i/(4m_n + m_\alpha)$ and $\boldsymbol{x}_i = \boldsymbol{r}_i + \boldsymbol{x}_\alpha$ of the core and neutrons relative to the projectile c.m. and the impact parameters b_j of each constituent can then be computed. In each such configuration f_{corr} is calculated and the $S_j(b_j)$ are interpolated from a pre-calculated lookup table. The form of the COSMA wavefunction and calculation outlined above shows that we include explicitly both angular and antisymmetrisation correlations and c.m. correlations associated with the finite mass of the α core; imposed by the vector relationships between the $\boldsymbol{x}_i$ and $\boldsymbol{x}_\alpha$.

4.2. Results of calculations

We apply the formalism above to the scattering of ^{8}He from ^{12}C at 60 MeV per nucleon. The additional inputs required are an α+^{12}C and a n+^{12}C interaction. The n+^{12}C potential used is that tabulated in [8] and used previously for ^{11}Li [8] and ^{11}Be [11] scattering at similar energies. For the α+^{12}C system we use a density dependent double folding model interaction [24] calculated using the BDM3Y1 effective interaction [21].

The measured ^{8}He+^{12}C angular distribution is quasielastic and includes events in which the ^{12}C target is inelastically excited. These contributions must be estimated theoretically and added to the calculated elastic cross section to make a comparison with the data. The cross sections to the 2^+ and 3^- states of ^{12}C are estimated in DWBA assuming rotational model couplings [8] and deformation lengths $\delta_2 = 1.648$ fm and $\delta_3 = 1.00$ fm [25].

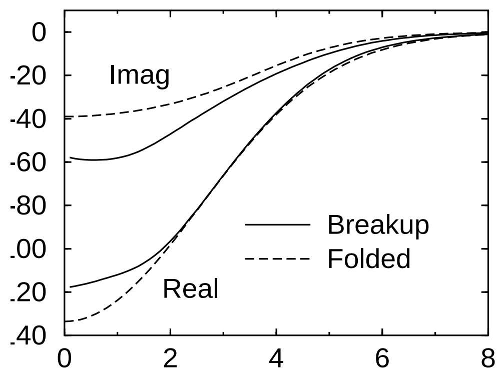

Figure 3. ^{8}He+^{12}C interactions.

The ^{8}He+^{12}C effective interaction used in the DWBA was calculated numerically from the deduced FB eikonal phase $\chi_8(b) = -i \ln S_8(b)$ using Eq. (7) of [26]. Its real and imaginary formfactors are shown by the solid curves in Figure 3. The absorptive potential is seen to be large, of order 60 MeV deep, to be compared with the α potential absorption of only 22 MeV. The importance of the breakup degrees of freedom are evident upon comparing this effective ^{8}He potential (in particular the absorption) with that obtained from the folding model (the no breakup limit) shown by the dashed curves in the Figure.

The elastic and 2^+ and 3^- inelastic scattering angular distributions (ratio to Rutherford) calculated using the FB model are shown by the long dashed, dot-dashed and short dashed curves in Figure 4. The sum, shown by the solid curve, can be compared with the data. We observe that the magnitude and forward angle oscillations in the data are reasonably reproduced and that the inelastic channel contributions are important to generating a cross section of the required magnitude at the larger angles. More extended investigation reveals [21] that the calculations show considerable sensitivity to a correct treatment of the c.m. correlations in the composite projectile. Accurate elastic rather than quasielastic scattering data at similar energies are needed to assess these quantitative theoretical questions further.

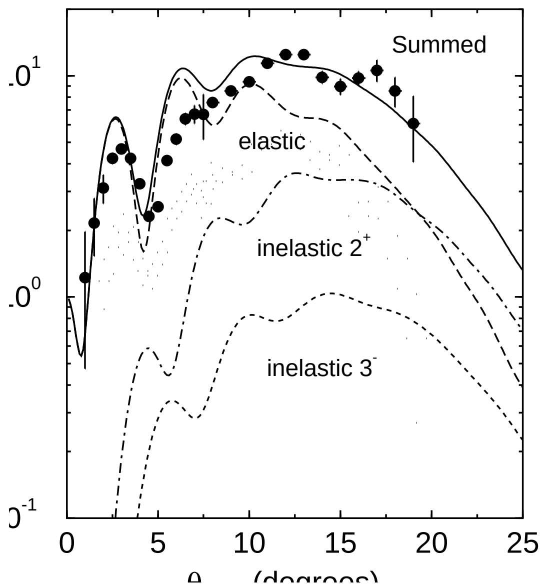

Figure 4. Experimental and calculated ^{8}He+^{12}C cross sections at 480 MeV. The curves show the elastic, inelastic and summed quasielastic calculations.

This example shows that the eikonal model provides a rather effective basis for the calculation of reactions of few-body projectiles. This efficiency arises from the use of the adiabatic approximation and also the very simple form of each two-body eikonal phase and S-matrix. Given the efficiency of the method it is worthwhile to investigate leading order corrections to the model in an attempt to assess and extend its accuracy. In the following we outline such an assessment using a three-body system where fully non-eikonal (adiabatic) calculations are also possible.

5. GOING BEYOND THE EIKONAL APPROXIMATION

^{11}Be is a good example of a binary, ^{10}Be+n, single neutron halo nucleus and one for which there are preliminary elastic scattering data available. For a two-body projectile full quantum mechanical calculations which use the adiabatic approximation but not the additional eikonal assumption can be performed [5] and used to assess the importance of (non-eikonal) corrections to the lowest order theory. Calculated cross section angular distributions which include non-eikonal modifications will be shown to be accurate at larger scattering angles and at lower energies.

For the two-body (core+n) projectile the FB elastic amplitude is given by Eq. (5), but now $S_2(b) = \langle\Phi_0^{(2)}|\, S_c(b_c)S_n(b_n)|\Phi_0^{(2)}\rangle$. From Eq. (1), $S_j(b_j) = \exp[i\chi_j(b_j)]$ $(j = c, n)$ where χ_c and χ_n are the eikonal phases for the core- and n-target subsystems.

Following Wallace [27] we use a correspondence between the eikonal phase and an expansion of the WKB phase shift. The latter, χ_j^{WKB}, can be expressed as an expansion in powers of $\epsilon = 1/\hbar K v$ about the eikonal phase

$$\chi_j^{WKB}(b) = \sum_{n=0}^{\infty} \frac{\epsilon^n}{(n+1)!}\, \chi_j^n(b) \ , \quad \chi_j^n(b) = -\frac{1}{\hbar v}\int_{-\infty}^{\infty} dz \left(\frac{1}{r}\frac{d}{dr}\right)^n [r^{2n}\, V_j^{n+1}(r)] \ , \tag{7}$$

which appears as the lowest order $n = 0$ term [28]. These χ_j^{WKB} are not exact and the required correction terms were clarified by Rosen and Yennie (RY) [29]. Our prescription for improving the phases in the FB model is to replace the eikonal phase for each particle j by [11]

$$\chi_j \ \rightarrow \chi_j^{WKB} + \chi_j^{RY} \quad , \tag{8}$$

where the second term accounts for the RY corrections, also expressed as an expansion in powers of ϵ. The treatment of the Coulomb interaction is discussed in detail in [11]. The generalisation of the method to many-body systems is obvious since the corrections proposed retain the independent scattering feature of the lowest order theory.

We apply this formalism to the ^{11}Be+^{12}C system and compare our non-eikonal calculations with exact adiabatic solutions of the three-body Schrödinger equation. The ^{11}Be ground state wavefunction was taken to be a pure $2s_{1/2}$ neutron single particle state, with separation energy 0.504 MeV, calculated in a central Wood-Saxon potential of geometry $r_0 = 1.00$ fm and $a_0 = 0.53$ fm. Assuming a ^{10}Be core rms matter radius of 2.28 fm this generates a ^{11}Be composite with rms radius of 2.90 fm [2].

Figure 5 shows the calculated elastic differential cross section angular distributions (ratio to Rutherford) for ^{11}Be+^{12}C scattering at 49.3 MeV per nucleon together with the GANIL data. The dashed curve shows the cross section in the absence of breakup contributions: the scattering solution for the single folding model interaction. The dot-dashed curve shows the results of the conventional (lowest order) eikonal model calculation, which includes ^{11}Be excitation and breakup channels. The results obtained when including the non-eikonal corrections to the core (^{10}Be) and neutron phases are shown by the long-dashed curve which are seen to agree to high precision with the exact adiabatic model calculations, presented by the solid curve.

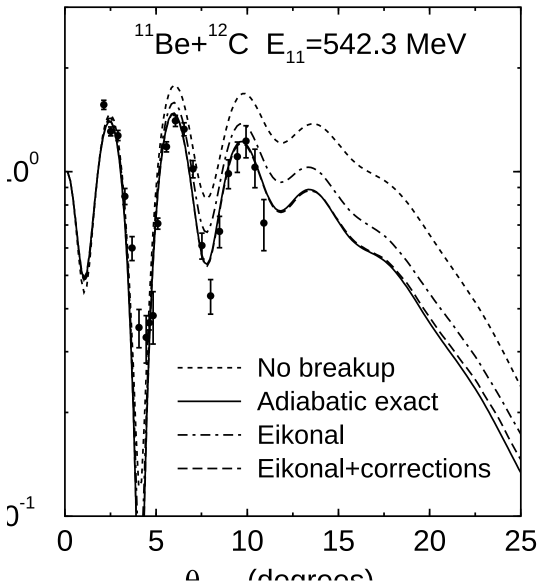

Figure 5. Calculated and experimental ^{11}Be+^{12}C cross sections at 49.3 MeV per nucleon.

These calculations include WKB and RY correction terms up to $n = 3$ in Eq. (7). At this order in ϵ other sources of non-eikonal corrections arise which destroy the simplicity associated with the independent scattering picture of the process. It is therefore inappropriate to include higher order WKB and RY terms without due consideration of these correlated scattering terms.

Several points are evident: (*i*) projectile excitation and breakup effects are large, (*ii*) at energies of order 50 MeV per nucleon there are already discrepancies between exact and eikonal model calculations at the scattering angles displayed which are typically greater than the error bars already achieved on the experimental data, (*iii*) the inclusion of non-eikonal corrections improves the accuracy of the calculated observables. This is achieved at a small fraction of the computational cost of carrying out the full partial wave, coupled channels, solution of the adiabatic Schrödinger equation.

Figure 6 presents similar calculations for incident ^{11}Be energy to 25 MeV per nucleon where the non-eikonal effects are larger. We note the continued success of the non-eikonal modifications to the few-body amplitude to correct the eikonal calculation very accurately over a significant range of scattering angles. Thus, a simple physical prescription which extends the range of applicability of eikonal model calculations for few-body systems is to include the WKB and RY corrections to the eikonal phase in each projectile constituent-target two-body channel, prior to the projectile ground state average being carried out. In the two-body projectile case this is shown to result in excellent agreement with exact adiabatic calculations for an expanded and useful range of c.m. scattering angles.

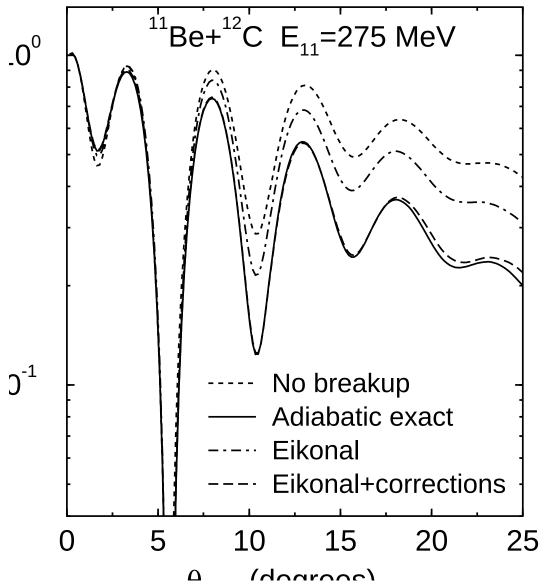

Figure 6. Calculated ^{11}Be+^{12}C cross sections at 25 MeV per nucleon.

A natural expectation, given the explicit spatial averaging in the composite projectile S-matrix in the eikonal model, is that this S-matrix, and hence the calculated cross section angular distributions, should reflect the spatial extent of the core-valence particle relative motion wavefunction. In Figure 7 we assess this sensitivity by showing the calculated elastic differential cross section angular distributions at 49.3 MeV/A for projectile wavefunctions with rms matter radii of 2.70 fm (long dashed curve), 2.90 fm (solid curve) and 3.10 fm (dot-dashed curve). The origin of this sensitivity has been clarified within the adiabatic model by Johnson *et al.* [30].

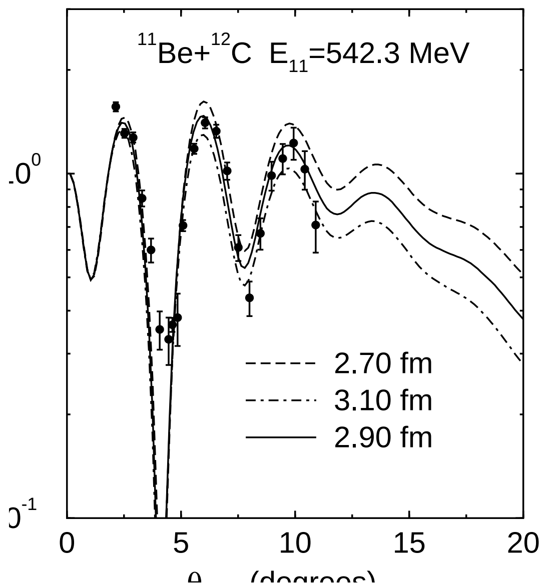

Figure 7. ^{11}Be+^{12}C cross sections for wavefunctions with different rms radii.

The model used, in which the core target interaction is assumed to dominate, is reported in a contribution to this meeting [30].

6. SUMMARY AND CONCLUSIONS

In this paper we have considered the way in which, for halo nuclei, nucleus-nucleus total reaction cross sections and elastic scattering differential cross section angular distributions require the few-body nature of the loosely bound composite structures to be treated explicitly. We have considered the optical limit and few-body approaches to the calculation of reaction cross sections and shown that the OL theory consistently overestimates calculated cross sections and hence underestimates the nuclear size determined from comparisons with experimental data.

We have also presented eikonal model calculations for ^{8}He scattering. The approach used makes such six-body calculations practical by exploiting the simplicities brought about by the eikonal and adiabatic treatment of the motions of the projectile constituents. The magnitude and angular distribution of the measured ^{8}He quasielastic cross section are found to arise naturally from the presented few-body model without parameter variation.

Finally we have proposed a simple physical prescription to enhance the accuracy and extend the range of applicability of the eikonal model calculations for few-body systems. The enhancement retains the essential simplicity of the eikonal model calculations, the independent scattering of the constituent particles, but leads to significantly more accurate calculations in the case of ^{11}Be scattering considered here. The corrections can be simply incorporated for more complex systems, such as the ^{8}He case considered here, and in the calculation of breakup momentum distributions and other experimental observables.

The author gratefully acknowledges the theoretical contributions of J.S. Al-Khalili, J.M. Brooke and I.J. Thompson, and the experimental contributions of M.D. Cortina-Gil, P. Roussel-Chomaz (for the ^{11}Be data), M. Zahar, M. Belbot, J.J. Kolata, K. Lamkin D.J. Morrissey, B.M. Sherrill, M. Lewitowicz and A.H. Wuosmaa (for the ^{8}He data) to this work.

REFERENCES

1. J.S. Al-Khalili and J.A. Tostevin, Phys. Rev. Lett. **76** (1996) 3903.
2. J.S. Al-Khalili, J.A. Tostevin and I.J. Thompson, Phys. Rev. C **54** (1996) 1843.
3. J.A. Tostevin and J.S. Al-Khalili, Nucl. Phys. **A616** (1997) 418c.
4. M. Yahiro *et al.*, Prog. Theor. Phys. Suppl. **89** (1986) 32.
5. H. Amakawa, S. Yamaji, A. Mori and K. Yazaki, Phys. Lett. **B82** (1979) 13.
6. J.A. Christley *et al.*, *Four-body adiabatic model applied to elastic scattering*, Nuclear Physics A, in press.
7. K. Yabana *et al.*, Phys. Rev. C **45** (1992) 2909; Nucl. Phys. **A539** (1992) 295.
8. J.S. Al-Khalili, I.J. Thompson and J.A. Tostevin, Nucl. Phys. **A581** (1995) 331.
9. Y. Ogawa *et al.*, Nucl. Phys. **A571** (1994) 784; Nucl. Phys. **A588** (1995) 77c.
10. M.M. Obuti *et al.*, Nucl. Phys. **A606** (1996) 74; Y. Ogawa and I.Tanihata, Nucl. Phys. **A616** (1997) 239c.
11. J.S. Al-Khalili, J.A. Tostevin and J.M. Brooke, Phys. Rev. C **55** (1997) R1018.

12. I.J. Thompson *et al.*, Nucl. Phys. **A588** (1995) 59c.
13. R.J. Glauber, *Lectures in Theoretical Physics*, (Interscience, N.Y., 1959) Vol. 1, 315.
14. I. Tanihata *et al.*, Phys. Lett. **B160** (1985) 380.
15. I. Tanihata *et al.*, Phys. Lett. **B206** (1988) 592.
16. W. Czyz and L.C. Maximon, Ann. Phys. (N.Y.) **52** (1969) 59.
17. Victor Franco and Girish K. Varma, Phys. Rev. C **18** (1978) 349.
18. S. Kox *et al.*, Phys. Rev. C **35** (1987) 1678.
19. S.K. Charagi and S.K. Gupta, Phys. Rev. C **41** (1990) 1610.
20. T. Kobayashi *et al.*, Phys. Lett. **B232** (1989) 51.
21. J.A. Tostevin *et al.*, *Elastic and quasielastic scattering of* ^{8}He *from* ^{12}C, submitted to Physical Review C.
22. M. Zahar *et al.*, Phys. Rev. C **49** (1994) 1540; Phys. Rev. C **54** (1996) 1262.
23. M.V. Zhukov, A.A. Korsheninnikov and M.H. Smedberg, Phys. Rev. C **50** (1994) R1.
24. Dao T. Khoa and W. von Oertzen, Phys. Lett. **B342** (1995) 6.
25. J.J. Kolata *et al.*, Phys. Rev. Lett. **69** (1992) 2631.
26. J.S. Al-Khalili and J.A. Tostevin, Phys. Rev. C **49** (1994) 386.
27. S.J. Wallace, Phys. Rev. D **8** (1973) 1846.
28. S.J. Wallace, Ann. Phys. (N.Y.) **78** (1973) 190; Phys. Rev. Lett. **27** (1971) 622.
29. M. Rosen and D.R. Yennie, J. Math. Phys. **5** (1964) 1505.
30. R.C. Johnson *et al.*, *Elastic scattering and elastic breakup of halo nuclei*, submitted to Physical Review Letters: R.C Johnson, contribution to this meeting.